The Fourth Member of the Tubular Family $[Bi_2Sr_2CoO_6]_n[Sr_8Co_6O_{16-\delta}]$: $Bi_{5.8}Sr_{15.2}Co_{10}O_{40-\delta}$

A. C. Masset, D. Pelloquin, A. Maignan, M. Hervieu, C. Michel,* and B. Raveau

Laboratoire CRISMAT, CNRS UMR 6508, ISMRA, 6, Boulevard du Maréchal Juin, 14050 Caen Cedex, France

Received May 18, 1999. Revised Manuscript Received September 10, 1999

A new cobaltite, $Bi_{5.8}Sr_{15.2}Co_{10}O_{40-\delta}$, with a tubular structure derived from the 2201-type has been synthesized. This oxide represents the $n = 4$ member of the large structural $[Bi_2Sr_2MO_6]_n[Sr_8M_6O_{16\pm\delta}]$ family (M = Cu, Mn, Co). Its average structure, similar to that of the copper-based phase, crystallizes in the space group *Fmmm* with cell parameters $a = 5.4650(5)$ Å, $b = 34.042(2)$ Å, and $c = 23.574(1)$ Å. Its complex crystal chemistry has been studied using XRPD and HREM techniques. This structure can be described as an intergrowth along *b*, of two types of (010) slices: "2201"-type slices $[Bi_2Sr_2CoO_6]$ that are four octahedron thick and cobalt-deficient perovskite-related slices $[Sr_8Co_6O_{16-\delta}]$ that are one octahedra thick. The study of the magneto-transport properties of this new cobaltite shows an antiferromagnetic behavior below 80 K and a large decrease by 500 of the resistivity at room temperature by annealing under oxygen pressure.

Introduction

After the report of the first oxide with a tubular structure $Bi_8Sr_{16}Cu_{10}O_{40-\delta}$, by Fuertes et al.,[1] the exploration of the system Bi−Sr−Cu−O has allowed a large structural family to be synthesized, derived from the layered superconductor $Bi_2Sr_2CuO_{6+\delta}$, with the generic formula $[Bi_2Sr_2CuO_6]_n[Sr_8Cu_6O_{16-\delta}]$ ($n = 4$, 5, 6, and 7).[2] Recently, the extended study of the Bi−Sr−M−O systems has demonstrated the ability of such original frameworks to be stabilized with other transition elements, such as manganese and cobalt.[3,4] These materials can be described as the intergrowth of two types of slices along the *b* direction. Typical 2201-type $Bi_2Sr_2MO_6$ ribbons *n* octahedra wide separated by an original layer $[Sr_8M_6O_{16-\delta}]$ related to the perovskite structure are running along *c*. Such a stacking induces criss-crossing monolayers of MO_p polyhedra, forming tubes where the [BiO] rows are located. At the intersection of two perpendicular monolayers, this framework forms oxygen deficient pillars built up of four MO_p polyhedra, whose nature (geometry and oxygen content) depends on M. The stability of these compounds is also closely dependent on the nature of M. For example the $n = 2$ member of the series can be easily synthesized with M = Mn, Co[3,4] with a mean valency ranging from +2.5 to +3 while it has never been observed to date in the case of copper whose usual oxidation state is close to +2. Moreover the magnetic and transport properties are complex and very sensitive to the oxygen content especially for the cobalt-based tubular structures. In this respect, the study of other members of the series ($n > 3$) with M = Co and Mn represents a promising alternative to clarify the factors which govern the stabilization of such frameworks and to synthesize new materials with potential interesting physical properties. This paper evidences the possibility to stabilize a new bismuth cobaltite, $Bi_{5.8}Sr_{15.2}Co_{10}O_{40-\delta}$, related to $[Bi_2Sr_2CoO_6]_n[Sr_8Co_6O_{16+\delta}]$ tubular family. This new cobaltite, corresponding to the $n = 4$ member of the tubular series, is especially described from HREM images while X-ray and chemical analyses have also been performed to compare it to the homologous cuprate $Bi_8Sr_{16}Cu_{10}O_{40-\delta}$.[1] In contrast, all attempts to isolate the homologous bismuth-pure manganite have failed.

Experimental Section

The Bi−Sr−Co−O system was investigated with starting compositions close to ideal composition expected for the $n = 4$ member of the tubular-type oxides i.e., $Bi_{8-x}Sr_{16}Co_{10}O_{40-\delta}$, *x* varying from 0 to 2.4 and δ from −2 to 4.5, respectively. All the samples were prepared by solid-state reaction among Bi_2O_3, SrO_2/SrO, and Co_3O_4/Co precursors weighted in the adequate proportions to give the expected δ value. To avoid the carbonate contamination, SrO oxide was freshly prepared by heating SrO_2 or $Sr(OH)_2{\cdot}8H_2O$ at 1000 °C. The mixtures, intimately ground in an agate mortar, were placed in an alumina finger. This step was performed in a drybox. Next the mixtures were sealed in an evacuated silica ampule and heated to a temperature close to 950 °C, at 150 °C h^{-1}, kept at this temperature for 24 h, and cooled to room temperature, at 150 °C h^{-1}. In a similar way, the progressive substitution of Mn or Ni for Co in the $n = 4$ tubular was studied.

The electron diffraction (ED) studies were carried out using a JEOL 200CX microscope, fitted with an eucentric goniometer (±60°), whereas the high-resolution electron microscopy (HREM) images were performed with a Topcon 002B microscope operating at 200 kV and having a point resolution of 1.8 Å. Both microscopes are equipped with EDS analyzers. HREM image calculations were carried out with the Mac-Tempas multislice program.

(1) Fuertes, A.; Miratvilles, C.; Gonzalez-Calbet, J.; Vallet-Regi, M.; Obradors, X.; Rodriguez-Carjaval, J. *Physica C* **1989**, *157*, 525.
(2) Caldes, M. T.; Hervieu, M.; Fuertes, A.; Raveau, B. *J. Solid State Chem.* **1992**, *97*, 48.
(3) Pelloquin, D.; Michel, C.; Maignan, A.; Hervieu, M.; Raveau, B. *J. Solid State Chem.* **1998**, *138*, 703.
(4) Pelloquin, D.; Masset, A. C.; Maignan, A.; Michel, C.; Hervieu, M.; Raveau, B. *Chem. Mater.* **1999**, *11*, 84.

10.1021/cm9903024 CCC: $18.00
Published on Web 11/12/1999

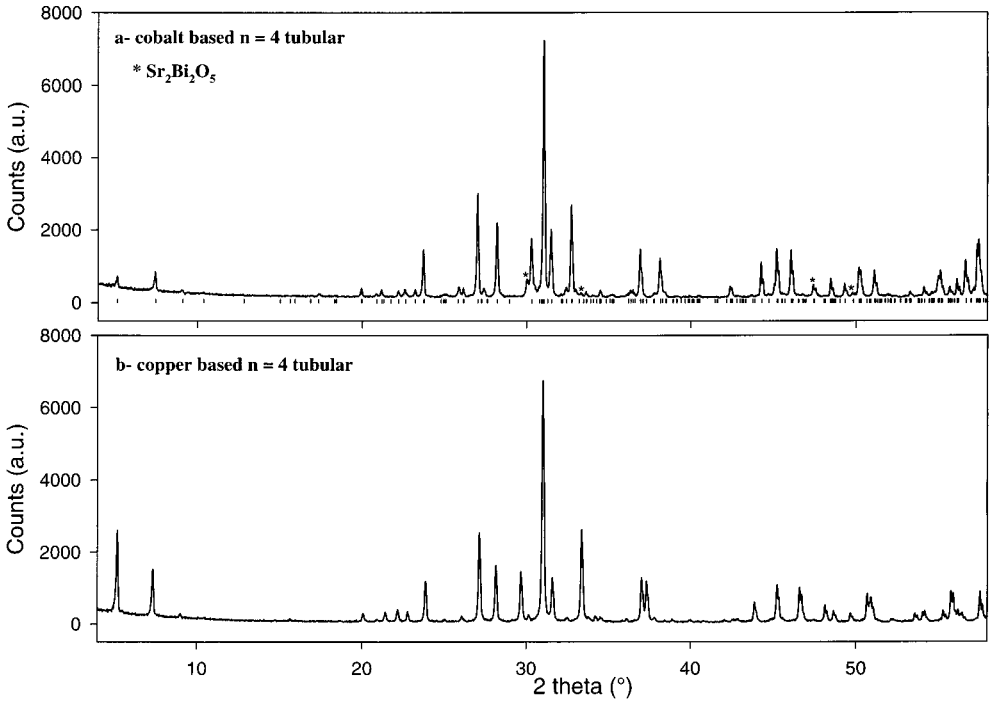

Figure 1. (a) Part of the experimental powder X-ray diffraction pattern of the tubular phase $Bi_{5.8}Sr_{15.2}Co_{10}O_{36.2}$. The vertical bars indicate the Bragg angle positions (space group *Fmmm*, $a = 5.4650(5)$ Å, $b = 34.042(2)$ Å, and $c = 23.574(1)$ Å. (b) Diffraction pattern calculated for the copper tubular-4 phase with positional parameters given in ref 1.

X-ray diffraction patterns were collected using a Philips vertical diffractometer, equipped with a secondary graphite monochromator and working with the Cu Kα radiation. Data collection was performed by step scanning over an angular range $5° \leq 2\theta \leq 100°$. The data were treated by profile analysis with the program Fullprof (version 3.2).[5]

Oxygen content was determined by chemical analyses using redox titration.

Magnetic susceptibilty $\chi(T)$ measurements were carried out at low temperature (5−400 K) using a Quantum Design SQUID magnetometer (ZFC process) and at high temperature (300−800 K) using a Faraday setup with, in both cases, an applied field of 3 kG. Resistivity measurements were recorded with a physical properties measurement system (PPMS) from Quantum Design (four-probe method). Electrical contacts were made of indium, ultrasonically deposited.

Results and Discussion

1. The Cobaltite $Bi_{5.8}Sr_{15.2}Co_{10}O_{40-\delta}$ ($\delta = 3.8$). For the above experimental conditions, a nearly pure sample has been obtained from the nominal composition $Bi_7Sr_{16}Co_{10}O_{40}$ ($x = 1$ and $\delta = 0$ in the formula $Bi_{8-x}Sr_{16}Co_{10}O_{40-\delta}$). The actual cationic composition deduced from EDS analyses and the oxygen content estimated from redox titration led in fact to a significantly different formula: $Bi_{5.8}Sr_{15.2}Co_{10}O_{36.2}$. This difference is easily explained by the formation of the $Bi_2Sr_2O_5$ phase[6] detected as an impurity both during the electron diffraction study and the X-ray powder pattern analysis. The latter (Figure 1a) shows clearly close relationships with the cuprate $Bi_8Sr_{16}Cu_{10}O_{40-\delta}$,[1] $n = 4$ member of the tubular family (Figure 1b). Thus this new cobaltite can be formulated as $Bi_{5.8}Sr_{15.2}Co_{10}O_{36.2}$, showing a significant bismuth and strontium deficiency with respect to the ideal formula. For comparison, the substitution of Mn for Co was attempted in this oxide, as well as the coupled Mn/Ni for Co substitution. The results, summarized in Table 1, show that only a part of cobalt can be replaced by manganese whereas the cobalt can be completely replaced by the couple Mn−Ni. Such a behavior is similar to that observed in the case of the $n = 2$ tubular cobaltite.[4]

Table 1. Analytical Results

ref	nominal composition	actual composition
this work	$Bi_7Sr_{16}Co_{10}O_{40}$	$Bi_{5.8}Sr_{15.2}Co_{10}O_{36.2}$
this work	$Bi_{7.2}Sr_{16}Co_{7.5}Mn_{2.5}O_{36.8}$	$Bi_{5.8}Sr_{16}Co_6Mn_4O_x$
this work	$Bi_{6.8}Sr_{15.6}Mn_{4.4}Ni_{5.6}O_{37.8}$	$Bi_{5.6}Sr_{16}Mn_6Ni_{4.6}O_x$
ref 1	$Bi_8Sr_{16}Cu_{10}O_{38+\delta}$	$Bi_{6.7}Sr_{16}Cu_{7.4}O_x$ (single crystal)

The reciprocal space for numerous crystallites was built by tilting about the crystallographic axes. The characteristic [100], [010], and [001] ED patterns (Figure 2) show that this oxide exhibits an orthorhombic cell with $a \approx a_p\sqrt{2} \approx 5.5$ Å (a_p is the parameter of the cubic perovskite-type structure), $b \approx 34$ Å and $c \approx 23.6$ Å $\approx c_{2201}$ (c_{2201} being the periodicity of the layer stacking in the 2201-type structures). The conditions limiting the reflections are *hkl*: $h + k$, $k + l$, $l + h = 2n$, compatible with the space groups *Fmmm*, *Fmm*2, and *F*222. The refinement of the cell parameters in the space group *Fmmm*, from the X-ray diffraction data (Figure 1), leads to the following values: $a = 5.4650(5)$ Å, $b = 34.042(2)$ Å, and c = 23.574(1) Å. These lattice parameters, compared to those obtained from single-crystal X-ray data ($a = 5.373(2)$ Å, $b = 33.907(6)$ Å, $c = 23.966(4)$ Å) for the copper tubular-4 phase, support the close relationships between this compound and the $n = 4$ tubular cuprate $Bi_8Sr_{16}Cu_{10}O_{40-\delta}$ [1] in agreement with the EDS analyses.

(5) Rodriguez-Carjaval, J. *Collected Abstract of Powder Diffraction meeting*; Galy, J., Ed. 1990; p 127.

(6) Guillermo, R.; Conflant, P.; Boivin, J. C.; Thomas, D. *Rev. Chim. Miner.* **1978**, *15*, 153. Vente, J. F.; Helmholdt, R. B.; Ijdo, D. J. W. *Acta Crystallogr.* **1992**, *C48*, 1380.

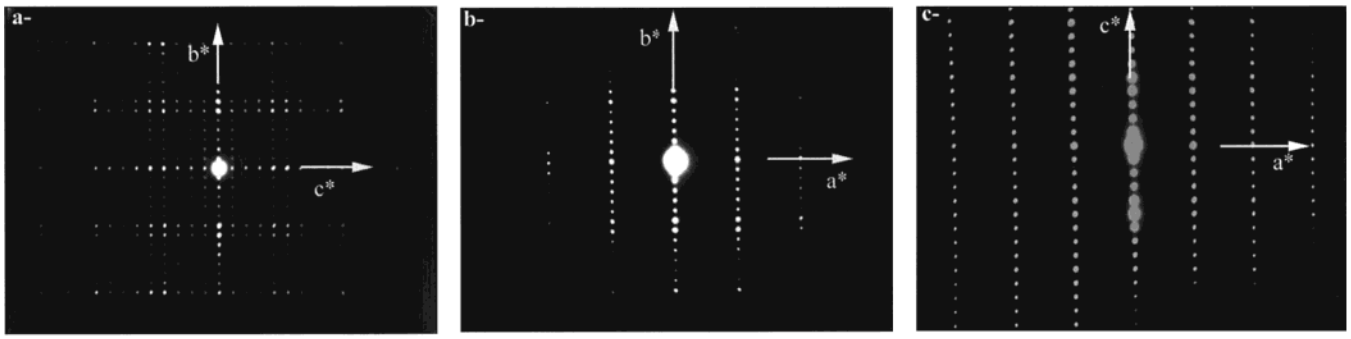

Figure 2. Experimental ED patterns oriented [100], [010], and [001] corresponding to $Bi_{5.8}Sr_{15.2}Co_{10}O_{36.2}$.

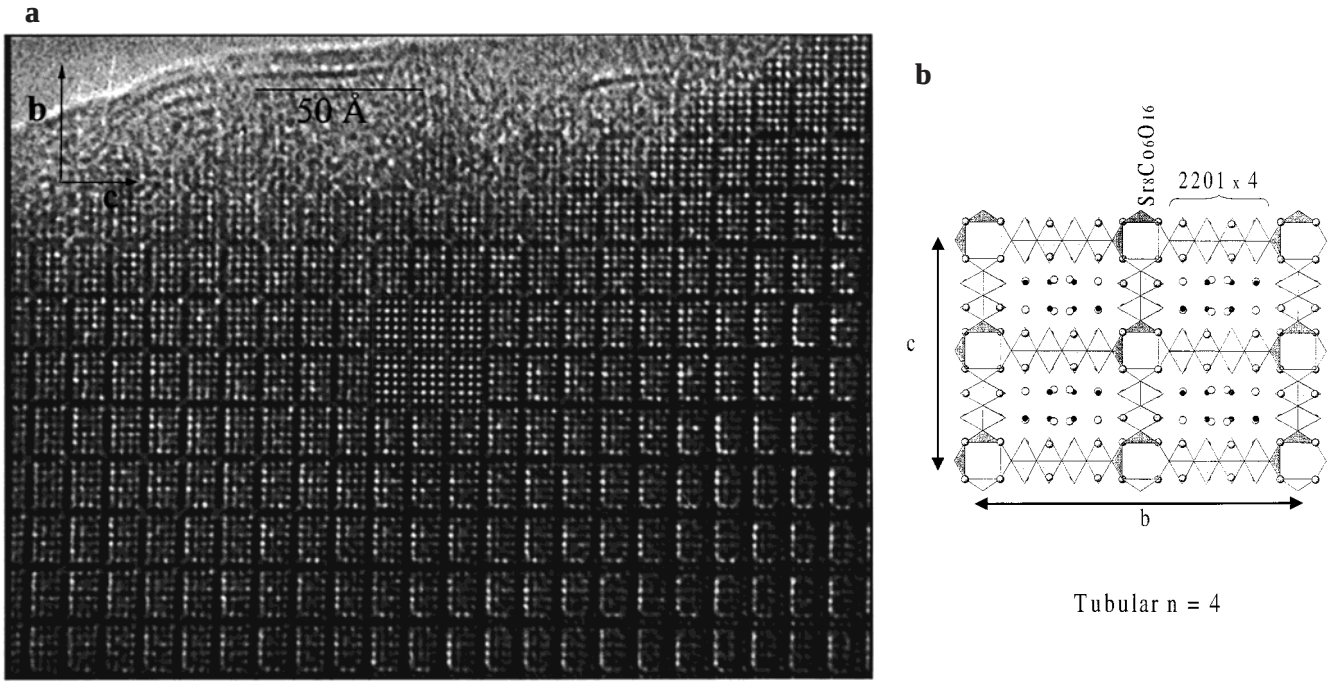

Figure 3. (a) Experimental and calculated (from structural parameters issue to $n = 4$ tubular cuprate study [1] with a defocus value = −550 Å and a thickness = 21 Å) HREM images recorded along [100] direction and (b) projection of the idealized model of the "tubular-4" structure.

Taking into account the great number of variable parameters involved by the high cell volume (≈ 4400 Å^3), no structural calculations were carried out from XRPD data. The structural analysis has only been performed by means of high-resolution techniques, comparing the experimental and calculated images from structural parameters refined for the homologous $n = 4$ tubular cuprate.[1] A typical $[100]_p$ HREM image is shown in Figure 3a, where the zones of high electron density are imaged as bright dots. The contrast consists of a rectangular paving of 6 × 4 bright dots rectangles, separated by perpendicular criss-crossing rows of gray dots. Referring to the HREM images previously recorded for the $n = 2$ member tubular cobaltite [4] and the $n = 4$ member tubular cuprate[1] and the simulated image (inset in Figure 3a) from the atomic positions of the latter, the intense bright dots can be correlated to the positions of Bi and Sr atoms and the gray ones to the cobalt positions. The great similarity of these images to those previously observed for the $n = 4$ member tubular cuprate[1] confirms the isotypism between the two structures. The schematized projection in the (*bc*) plane of this new tubular cobaltite $Bi_{5.8}Sr_{15.2}Co_{10}O_{36.2}$ (Figure 3b) shows its great similarity with the 2201 type structure. One recognizes the existence of 2201-type slices parallel to (010), which are four CoO_6 octahedra wide along *b*, i.e., involving four $[BiO]_\infty$ double rows running along *a*. Such slices which are four cobalt octahedra wide can be formulated $[(Bi_2Sr_2CoO_6)_4]_\infty$. On both sides of each slice along *b*, the propagation of the cobalt octahedral layer is interrupted by oxygen vacancies, leading to the formation of CoO_p distorted polyhedra. It results in the formation of square pillars formed by four CoO_p polyhedra: such pillars are connected through rows of four CoO_6 octahedra belonging to the $[(Bi_2Sr_2CoO_6)_4]_\infty$ slices along *b*, whereas they are connected through rows of two CoO_6 octahedra along *c*. So, the $[(Bi_2Sr_2CoO_6)_4]_\infty$ slices are separated along *b* by blocks $Sr_8Co_6O_{16-\delta}$ related to the perovskite structure. The HREM images recorded along [001] and [010] directions with a defocus value close to that of Figure 3a, i.e., the zones of high electron density are lightened, are given in Figure 4 and illustrate clearly the periodicity observed along both directions. Note that for these two orientations no direct correlation with the atomic arrangement can be made, owing to the mean projection of the cations (Bi, Sr, and Co) belonging to the different layers. The HREM image shown in Figure 4a, corre-

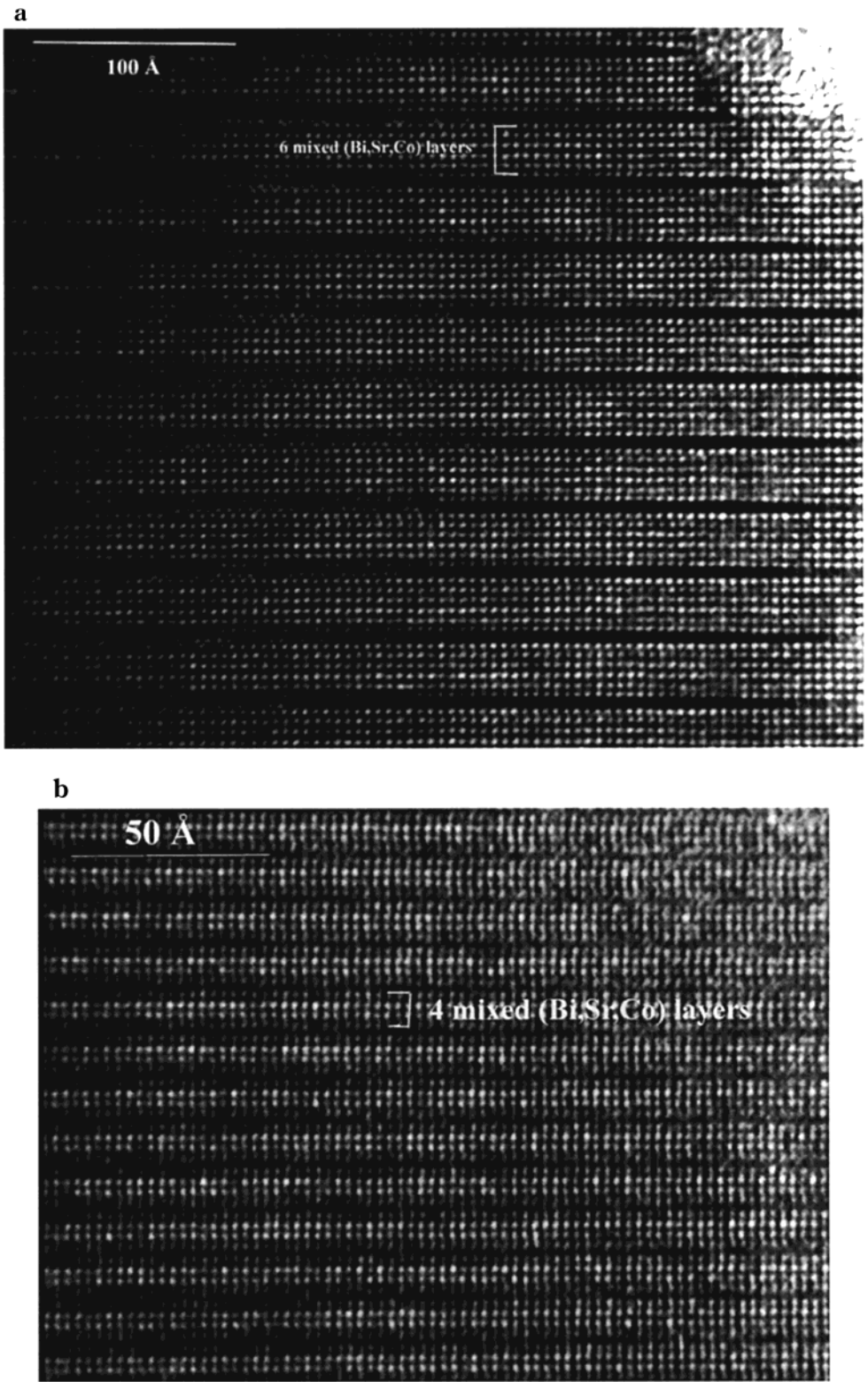

Figure 4. Experimental HREM image recorded along [001] (a) and [010] (b) for $Bi_{5.8}Sr_{15.2}Co_{10}O_{36.2}$.

sponding to [001]-oriented crystals, evidences in the edge of crystal some blocks of six rows of bright dots spaced by one row of gray dots. In the thicker zone, the six rows of bright dots split up into four successive lighted rows and two adjacent dimmer rows. Such contrasts correspond to the stacking of four mixed (010) [Bi,Sr,Co] layers with two mixed (010) [Sr,Co] layers alternatively in agreement with the view of the structure along *c* (Figure 3b). A similar description can be performed for the HREM image corresponding to [010]-oriented crystals (Figure 4b) where only the size of the blocks changes. Each row of gray dots is indeed isolated by four, instead of six, rows of bright dots also correlated to mixed (Bi,Sr,Co) layers. The two types of groups of bright dots are systematically separated by one row of gray dots correlated to pure cobalt layers in agreement with the view of the structure along *b* (Figure 3b).

The important information provided by theses images is the great regularity of the layers stacking in the different directions and the absence of local ordering or

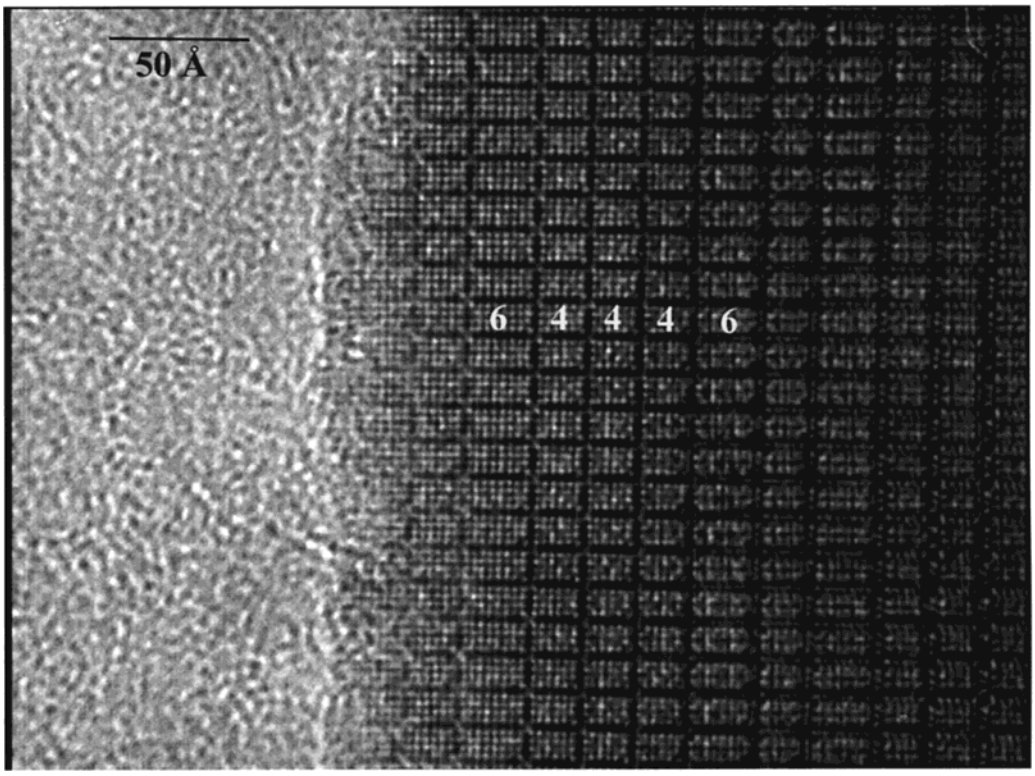

Figure 5. Experimental HREM image recorded along [100] for the mixed Mn−Ni $n = 4$ tubular phase.

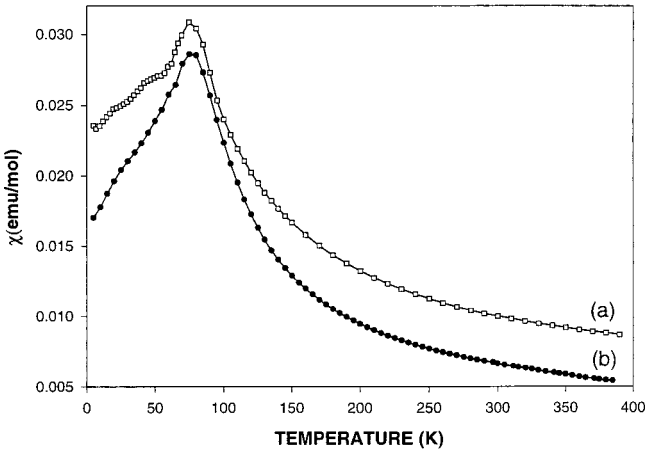

Figure 6. Temperature dependence of the molar susceptibility χ_M for the as-synthesized (a) $n = 2$ and (b) $n = 4$ tubular cobalt phases.

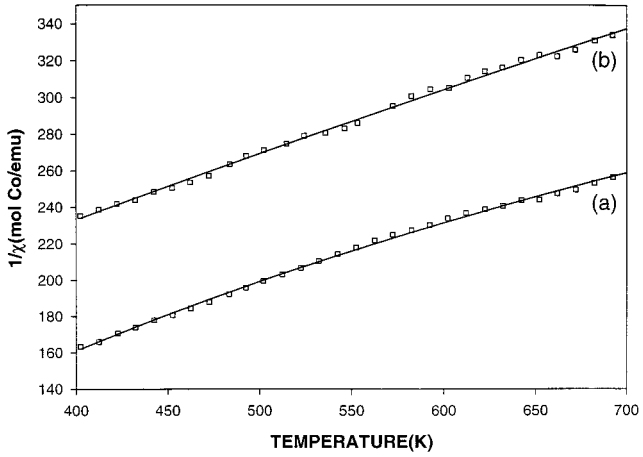

Figure 7. Temperature dependence of the inverse magnetic susceptibility per cobalt atom for the as-synthesized (a) and oxygen pressure annealed (b) tubular-4 cobaltite. Open squares are the experimental points and solid lines the curve fits.

modulation phenomenon. In fact, only isolated stacking defects, corresponding often to the $n = 6$ member, as illustrated in Figure 5, have been observed in the case of the mixed nickel−manganese $n = 4$ tubular.

2. Magneto-transport Characteristics. The magnetic susceptibility $\chi(T)$ measurements performed in the range 5−800 K show that this new cobaltite exhibits complex magnetic properties. This point is illustrated in Figure 6 where the T-dependent susceptibility χ curve of the as-synthesized $n = 4$ member is compared to that of the homologeous $n = 2$ member. Both $\chi(T)$ curves are characterized by a transition toward a less magnetic state below 80 K. Although this cobaltite does not show a pure Curie−Weiss behavior, the fitting of the corresponding $\chi^{-1}(T)$ curve in the temperature range (400−700K) (Figure 7), according to the general formula $\chi = \chi_0 + C/(T - \theta_p)$ (where χ_0, C, and θ_p are the temperature-independant susceptibility, the Curie constant, and the paramagnetic Curie temperature respectively), leads to $\theta_p = 116$ K and an effective paramagnetic moment of 2.9 μ_B per Co in the case of the as-synthesized sample and $\theta_p = -154$ K and $\mu_{eff} = 3.6\ \mu_B$ in the case of oxygen pressure annealed sample ($PO_2 = 100$ b, $T = 450$ °C:24 h). These μ_{eff} values are close to those observed in the same temperature range for the as-synthesized tubular $n = 2$ $Bi_{3.7}Sr_{11.4}Co_8O_{26.8}$ ($\mu_{eff} = 3.4\ \mu_B$).[4] Though the μ_{eff} values of cobalt should be interpreted cautiously, a formal valence close to +2.5 for cobalt has been proposed for the as-synthesized $n = 2$ member taking into consideration chemical and structural analyses that evidence two kinds of CoO_p polyhedra (50% of octahedra and 50% of tetrahedra). Such a hypothesis, i.e., an intermediate valence state, may also be considered for

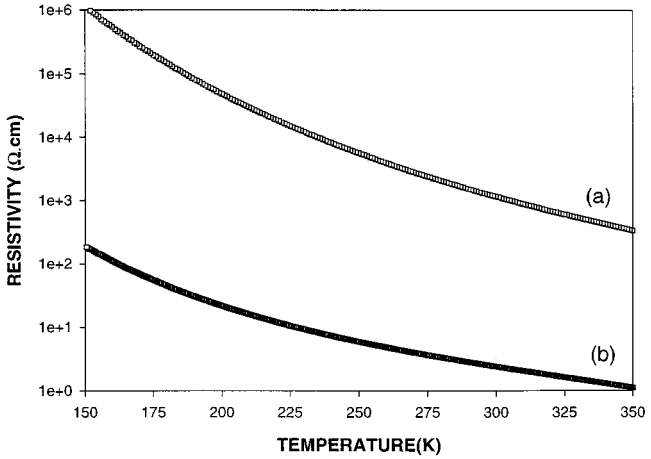

Figure 8. $\rho = f(T)$ curves for the as-synthesized (a) and oxygen pressure annealed (b) tubular-4 cobaltite.

this new member of cobalt-based tubular family taking into account the structural model (see Figure 3b) that implies also two different polyhedra for cobalt (60% of Co belongs to pure perovskite slices and 40% of CoO_p forms pillars) and the results obtained by chemical analyses, $Bi_{5.8}Sr_{15.2}Co_{10}O_{36.2}$ and $Bi_{5.8}Sr_{15.2}Co_{10}O_{37}$ before and after oxygen annealing, that have led to a mean oxidation state close to +2.4 and +2.6, respectively. Nevertheless further oxygen pressure annealings in the same conditions did not allow the introduction of additional oxygen and the further increase in the oxidation state of cobalt. This is an unexpected result, if one takes into account the mean valence, close to +3, observed for the $n = 2$ tubular phase after a similar oxygen pressure annealing. This difference in behavior may be due to the large cationic deficiency ($Bi_{5.8}Sr_{15.2}Co_{10}$ instead of the theoritical stoichiometry $Bi_8Sr_{16}Co_{10}$) systematically observed from EDS analyses. The $\chi(T)$ curve shape and the θ_p value suggest that an antiferromagnetic state occurs or that the Co spin-state changes toward a lower spin state. In contrast to the $n = 2$ tubular cobaltite, the annealings under oxygen pressure do not induce a second magnetic transition at high temperature (~450 K), suggesting that the latter is indeed correlated to an intermediate spin-state between Co(III-LS) and Co(+3-HS).

The resistivity curves $\rho(T)$ of the as-synthesized and oxygen pressure annealed $n = 4$ tubular phase are plotted in Figure 8. Both samples exhibit a semiconducting behavior obeying to an Arrhenius law. The activation energies, measured in the range from 150 to 350K, and room temperature resistivities are reported in Table 2 where they are compared to the $n = 2$ member. The two members of this tubular family are characterized by a large decrease of the resistivity after oxygen annealing, which can be correlated to the oxidation of cobalt due to oxygen uptake. In the same way, the activation energies decrease after oxygen annealing (Table 2).

Table 2. Room Temperature Resistivity and Activation Energy for Tubular-2 and -4 Samples

sample	ρ_{300K} (Ω cm)	E_a (meV)
$n = 2$ as-synthesized ($Bi_{3.7}Sr_{11.4}Co_8O_{26.8}$)	370	80
$n = 2$ PO_2 annealed ($Bi_{3.7}Sr_{11.4}Co_8O_{27.8}$)	2	14
$n = 4$ as-synthesized ($Bi_{5.8}Sr_{15.2}Co_{10}O_{36.2}$)	1150	80
$n = 4$ PO_2 annealed ($Bi_{5.8}Sr_{15.2}Co_{10}O_{37}$)	2.4	49

Concluding Remarks

This study has allowed a new cobaltite, member $n = 4$ of a large tubular family $[Bi_2Sr_2CoO_6]_n[Sr_8Co_6O_{16\pm\delta}]$, to be synthesized. It demonstrates that cobalt, like copper and manganese, is a potential element for the generation of tubular phases. The structure of this tubular phase, derived from the structure of the $Bi_2Sr_2CoO_{6.25}$ [7] (2201-type) oxide, owns an essential feature: the $[CoO_2]$ planes are periodically, all four octahedra, interrupted by other $[CoO_{2-\delta}]$ layers stacked perpendicularly to them. The most striking structural consequence of such mechanism is to generate tubes at the level of criss-crossing of cobalt layers and to delete the commensurate modulation, which is of periodicity 4 for the cobalt-based type-2201 compound.[7] Nevertheless the "mechanisms" which govern the stabilization of such frameworks are complex. For example, the $n = 3$ member of the tubular cobaltite family is not stabilized in these experimental conditions whereas the $n = 2$ and 4 members can be isolated. Moreover the nature of the transition element, in particular its usual mean oxidation state, seems an important parameter: the stabilization of the $n = 4$ member requires a M cation with a mean valence close to 2−2.5 as suggested by the present work and the results obtained in the case of M = Cu.[1] Such a value is not convenient in the case of manganese and nickel and could explain that attempts to synthesize the $n = 4$ pure manganite and nickelate tubular were unsuccessful.

Acknowledgment. The authors are grateful to Dr. N. Nguyen for susceptibility measurements at high temperature.

CM9903024

(7) Tarascon, J. M.; Micelli, P. F.; Barboux, P.; Hwang, D. M.; Hull, G. W.; Giroud, M.; Greene, L. H.; Le Page, Y.; McKinnon, W. R.; Tselepsis, E.; Neumann, D. A.; Rhyne, J. J. *Phys. Rev.* **1989**, *B39*, 11587.